Journal of Organometallic Chemistry 729 (2013) 68–80

Contents lists available at SciVerse ScienceDirect

Journal of Organometallic Chemistry

journal homepage: www.elsevier.com/locate/jorganchem

Crystal structure of $(CO)_3(CH_3)Mo[(\eta^5\text{-}C_5H_4)C(CH_3)=N-N=C(CH_3)(\eta^5\text{-}C_5H_4)]Mo(CO)_3(CH_3)$ and unequivocal assignments of C(2,5) and C(3,4) on the cyclopentadienyl ring of cynichrodene, tricarbonyl(η^5-cyclopentadienyl)methylmolybdenum, tricarbonyl(η^5-cyclopentadienyl)methyltungsten, ferrocene, and dicarbonyl(η^5-cyclopentadienyl)cobalt derivatives bearing an electron-withdrawing carbonyl substituent in ^{13}C NMR spectra

Yu-Pin Wang*, Wei-Der Tang, Hsiu-Yao Cheng, Tso-Shen Lin

Department of Chemistry, Tunghai University, Taichung 407, Taiwan, ROC

ARTICLE INFO

Article history:
Received 9 September 2012
Received in revised form
3 January 2013
Accepted 15 January 2013

Keywords:
Chromium
Molybdenum
Cobalt
Ferrocene
2D HetCOR–NMR
B3LYP

ABSTRACT

Schiff's bases (η^5-formylcyclopentadienyl)tricarbonylmethylmolybdenum 2,4-dinitrophenylhydrazone (**6**), (η^5-acetylcyclopentadienyl)tricarbonylmethylmolybdenum 2,4-dinitrophenylhydrazone (**7**), and (η^5-acetylcyclopentadienyl)tricarbonylmethylmolybdenum azine (**8**) were obtained from condensation reaction of $(CO)_3(CH_3)Mo(C_5H_4CHO)$ (**3**) or $(CO)_3(CH_3)Mo(C_5H_4COCH_3)$ (**4**) with each corresponding primary amine. The structures of **7** and **8** were determined by X-ray diffraction studies.

The chemical shifts of C(2)–C(5) carbon atoms of the series of substituted-cyclopentadienyl Cp(M) derivatives—$(CO)_2(NO)M[\eta^5\text{-}(C_5H_4COOCH_3)]$ (**1** M = Cr, **2** M = Mo), $(CO)_3(CH_3)Mo[\eta^5\text{-}(C_5H_4\text{-sub})]$ (**3**–**5**, **6**, **7**, **8**)—have been assigned using two-dimensional HetCOR NMR spectroscopy. The assigned chemical shifts were compared with the NMR data of other organometallic Cp(M) analogs, $(CO)_2(NO)CrCp$, $(CO)_3(CH_3)WCp$, Cp_2Fe, and $(CO)_2CoCp$. We observed that C(3,4) resonate at a lower field than C(2,5) in $(CO)_3(CH_3)Mo[\eta^5\text{-}(C_5H_4CHO)]$ **3** and **4**, whereas C(2,5) resonate at a lower field than C(3,4) in $(CO)_3(CH_3)Mo[\eta^5\text{-}(C_5H_4COOCH_3)]$ **5**. The correlation between the magnitudes of nonplanarity of Cp-exocyclic carbon to π-acceptor substituents and the extent of deshielding on the C(3,4) of the Cp ring was discussed. The electron density distribution in the cyclopentadienyl ring was discussed on the basis of ^{13}C NMR data and those of **4**, **7**, and **8** were compared with calculations using the density functional B3LYP exchange-correlation method.

1. Introduction

Previously, we reported the opposite correlation of the assignments of C(2,5) and C(3,4) on the Cp ring, in the ^{13}C NMR spectra, between cynichrodene and ferrocene derivatives bearing electron-withdrawing substituents [1]. In the case of Cp(M) derivatives bearing metals enriched with π-electrons—ferrocene, the 3,4-positions are more sensitive to the electron-withdrawing substituent, whereas in the case of Cp(M) bearing metals depleted with π-electrons—$(CO)_2(NO)CrCp$ (hereafter called cynichrodene), the 2,5-positions are more sensitive to the electron-withdrawing substituent. That the overall electron-withdrawing property of CO and NO ligands on the chromium atom of cynichrodene derivatives may exert the difference has prompted us to study molybdenum Cp derivatives: $(CO)_2(NO)MoCp$ and $(CO)_3(CH_3)MoCp$. Further, while the chemistry of dicarbonylcyclopentadienylnitrosyl complexes of molybdenum, **2** [2], and tricarbonylcyclopentadienylmethyl complexes of molybdenum, **3**–**5** [3], have been studied, ^{13}C NMR data of these complexes have not been reported in the literature.

The qualitative relationship of nonplanarity of Cp-exocyclic carbon to substituent π-donor and π-acceptor interactions has also been addressed [1]. The π-donor substituents and the ipso-carbon atoms to which they are attached are bent away from the

* Corresponding author. Tel.: +886 423591217; fax: +886 423590426.
E-mail addresses: ypwang@thu.edu.tw, ypwang403070@yahoo.com.tw (Y.-P. Wang).

0022-328X/$ – see front matter © 2013 Elsevier B.V. All rights reserved.
http://dx.doi.org/10.1016/j.jorganchem.2013.01.011

$Cr(CO)_2NO$ fragments, whereas the π-acceptor substituents and the ipso-carbon atoms to which they are attached are approximately in the Cp plane or are bent slightly toward the $Cr(CO)_2NO$ fragments. The magnitudes and directions of these distortions of the Cp planarity appear to be due primarily to electronic effects. In hope of confirming those hypotheses and probing the reasons behind those hypotheses, we compared the theta values from X-ray data and the extent of deshielding on C(3,4) of some selected Cp(M) organometallic compounds.

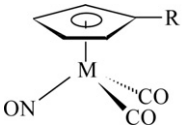

1 M = Cr, R = $COOCH_3$
2 M = Mo, R = $COOCH_3$

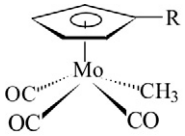

3 R = CHO
4 R = $COCH_3$
5 R = $COOCH_3$
6 R = CH=NHNH(2,4-$(NO_2)_2C_6H_3$)
7 R = CH=N(CH_3)NH(2,4-$(NO_2)_2C_6H_3$)

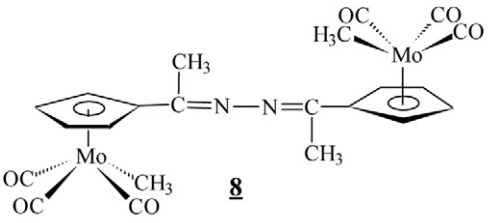

8

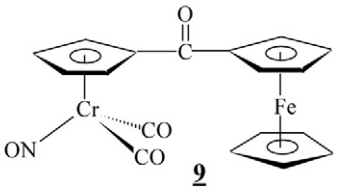

9

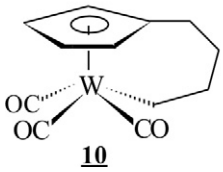

10

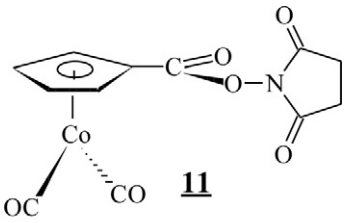

11

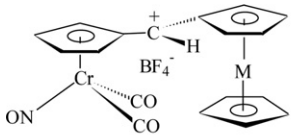

12 M = Fe
13 M = Ru

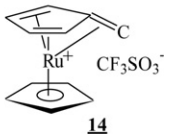

14

2. Results and discussion

Synthesis and characterization.

2.1. Synthesis

On exposure to 2,4-dinitrophenylhydrazine, $(CO)_3(CH_3)Mo(C_5H_4–CHO)$ **3** formed the corresponding hemiaminal, which readily lost water [4] in the presence of Lewis acid BF_3 to form an imine derivative **6** with a yield of 90%. Analogous reaction between ketone **4** and 2,4-dinitrophenylhydrazine or hydrazine gave compounds **7** and **8** in yields of 97% and 93%, respectively.

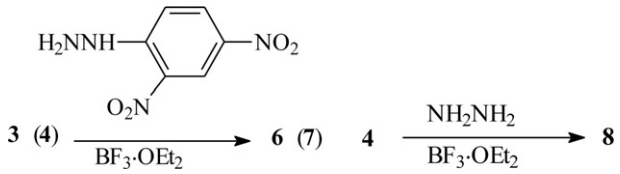

2.2. Characterization: IR

Table 1 [2,3,5–7] lists selected IR data for compounds **1**–**9**. The IR spectrum of **6** contained terminal metal carbonyl bands at 2020 and 1936 cm^{-1}, as well as a characteristic Schiff's bases' C=N stretching band at 1622 cm^{-1}. The two nitrosyl stretching bands were observed in the IR spectrum, the symmetric mode occurring at 1511 cm^{-1} and the asymmetric mode at 1337 cm^{-1}. Other functional groups showed their characteristic absorbances.

It is interesting to compare the carbonyl stretching vibrations among $-COCH_3$, $-CHO$, and $-COOCH_3$ groups. From Table 1, the following order of increasing wavenumbers of the organic carbonyl stretching was observed: $-COCH_3$ (1665 cm^{-1}) < $-CHO$ (1680 cm^{-1}) < $-COOCH_3$ (1710 cm^{-1}). This trend correlated well with the order of increasing tendency of the electron-withdrawing property given by: $-CH_3 < -H < -OCH_3$. The electron attracting property of the adjacent atom inductively attracts the electrons on the carbonyl oxygen, thus increasing the force constant of the C=O bond [8].

2.3. Characterization: ^1H NMR

The ^1H NMR spectra of compounds **6**–**8** are consistent with their assigned structures and are similar to other metallocenyl systems [2,3,5,9]. The ^1H NMR spectrum (Fig. 1) of **7** exhibited two singlets of relative intensity 1H owing to the H(3) of the phenyl group and the NH proton at $\delta = 8.85$ and $\delta = 11.0$, respectively, two singlets of relative intensity 3H owing to the Mo($C\underline{H}_3$) and the C($C\underline{H}_3$)=N at $\delta = 0.32$ and $\delta = 2.21$, respectively, two doublets of relative intensity 1H owing to the H(5) and the H(6) of the phenyl group at $\delta = 8.26$ and $\delta = 7.96$, respectively, and an A_2B_2 pattern related to the observed triplet. The downfield triplet can be assigned to the H(2,5) protons of the Cp(Mo) ring. This assignment was made on the basis of the fact that the iminyl group would exert a strong diamagnetic anisotropic effect and exhibit an electron-withdrawing property. As expected, H(2,5) would be deshielded to a greater extent than the protons on the more remote 3- and 4-positions. Accordingly, the following assignments were made: H(2,5) and H(3,4) of Cp(Mo) resonate at $\delta = 6.12$ and 5.71, respectively, for complex **7**. Similarly, H(2,5) and H(3,4) of Cp(Mo) for complexes **5** and **6** were assigned (Table 2).

2.4. Characterization: ^{13}C NMR

The assignments of ^{13}C NMR spectra for **2**–**8** (Table 3) were based on standard ^{13}C NMR [1,10], 2D HetCOR, and the DEPT correlation techniques. They were also compared with other metallo-

Table 1
IR spectra of **1**–**9**.

		ν(CO)		ν(NO)	−C(O)−	C=N
1	$(CO)_2(NO)CrCp$[a]	2020	1945	1680		
	$(CO)_2(NO)Cr(\eta^5\text{-}C_5H_4COOCH_3)$[a]	2024	1954	1695		
	$(CO)_2(NO)MoCp$[a]	2019	1946	1649		
2	$(CO)_2(NO)Mo(\eta^5\text{-}C_5H_4COOCH_3)$[a,d]	2025	1945	1720	1665	
	$(CO)_3(CH_3)MoCp$[c,e]	2018	1927			
3	$(CO)_3(CH_3)Mo(\eta^5\text{-}C_5H_4CHO)$[a,f]	2020	1920		1680	
4	$(CO)_3(CH_3)Mo(\eta^5\text{-}C_5H_4COCH_3)$[b,f]	2020	1920		1665	
5	$(CO)_3(CH_3)Mo(\eta^5\text{-}C_5H_4COOCH_3)$[a,f]	2010	1915		1710	
6	$(CO)_3(CH_3)Mo(\eta^5\text{-}C_5H_4$ $\{CH{=}NNH[2,4\text{-}(NO_2)_2C_6H_3]\}$[a]	2020	1936			1622
7	$(CO)_3(CH_3)Mo(\eta^5\text{-}C_5H_4$ $\{C(CH_3){=}NNH[2,4\text{-}(NO_2)_2{-}C_6H_3]\}$[a]	2019	1952, 1914			1615
8	$((CO)_3(CH_3)Mo\{\eta^5\text{-}C_5H_4[C(CH_3){=}N)_2$[b]	2015	1927			1606
9	$(CO)_2(NO)Cr(\eta^5\text{-}C_5H_4COC_5H_4)FeCp$[c, g]	2030	1965	1710	1630	

[a] KBr.
[b] Neat.
[c] In CH_2Cl_2.
[d] From Ref. [2].
[e] From Ref. [6].
[f] From Ref. [3].
[g] From Ref. [7].

aromatic systems [11]. In the case of **3**, four relatively less intense signals were observed at δ = 223.70, 235.94, 185.47, and 104.15 corresponding to the two terminal carbonyl carbons, the carbonyl carbon, and the C(1) of Cp(Mo), respectively. The line assignments for C(2−5) of Cp(Mo) were more difficult to make. Based on the 2D HetCOR results (Fig. 2), in which the magnetic fields of ^1H and ^{13}C NMR spectra increase toward the right and upper side, respectively, the upfield chemical shifts of C(2,5) correlate with the downfield chemical shifts of H(2,5) (δ = 5.70) and the downfield chemical shifts of C(3,4) correlate with the upfield chemical shifts of H(3,4) (δ = 5.51). Accordingly, chemical shifts at δ = 93.01 and 96.13 were assigned to C(2,5) and C(3,4) of Cp(Mo), respectively. Analogous assignments apply to complexes **4**, **6**, and **7**. These assignments

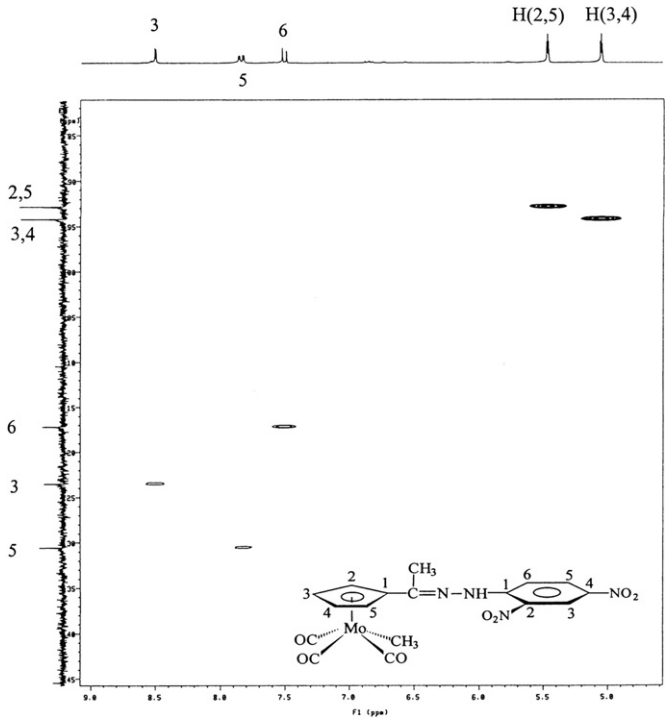

Fig. 1. 2D $^1H\{^{13}C\}$ HetCOR NMR spectrum of **7** in $CDCl_3$.

reveal that positions 3 and 4 on the substituted Cp ring in $(CO)_3(CH_3)MoCp$ are more sensitive to electron-withdrawing substituents, as are ferrocene analogs [12].

Fig. 3 shows the 2D $^1H\{^{13}C\}$ HetCOR NMR spectrum of **5**. Accordingly, chemical shifts at δ = 94.41 and 94.06 were assigned to C(2,5) and C(3,4) of Cp(Mo) of **5**, respectively. Similarly, chemical shifts of complexes **2** were assigned. These assignments reveal that the 2- and 5-positions of the substituted cyclopentadienyl ring are more sensitive to electron-withdrawing substituents in the cases of **2** and **5**, as are cynichrodene analogs [1]. This is contrary to the ferrocene analogs [12]. The 2D $^1H\{^{13}C\}$ HetCOR NMR spectrum of **9** [7], which is a complex containing both Cp(Cr) and Cp(Fe) moieties, is also shown (Fig. 4) for comparison. We note that the Cp(Cr) moiety exhibits a positive slope, whereas the Cp(Fe) moiety exhibits a negative slope.

3. Discussion

3.1. Electron-withdrawing effect of carbonyl substituents on Cp(M)

In Tables 4(a,b) and 5, ^{13}C NMR and ^1H NMR chemical shifts of a representative group of monosubstituted cynichrodene, $(CO)_3(CH_3)MoCp$, $(CO)_3(CH_3)WCp$, ferrocene, and $(CO)_2CoCp$ derivatives are presented, and Table 6 exhibits the contracted 2D HetCOR spectra of those complexes.

Upon examination of the ^{13}C NMR spectral data from Table 4a [13–17], the resonance-induced electron-withdrawing effect arranged in the same order of capability of deshielding the C(3,4) carbons is: −CHO > $-COCH_3$ > $-COOCH_3$, in all the selected Cp(M) derivatives, $(CO)_2(NO)Cr(C_5H_4R)$ (0.77 < 1.55 < 2.38); $(CO)_3(CH_3)Mo(C_5H_4R)$ (−3.12 < −1.82 < 0.35); $(CO)_3(CH_3)W(C_5H_4R)$(−4.01 < −2.59 < −0.28); $CpFe(C_5H_4R)$ (−4.6 < −2.6 < −1.2); and $(CO)_2Co(C_5H_4R)$ (−6.03 < −4.75 < −2.80). Since **Δr** is equal to δ[C(2,5)] − δ[C(3,4)], the larger negative value of **Δr** indicates a stronger deshielding effect exerted on the C(3,4). The formyl group withdraws the π electrons from Cp(M) more readily than the ester group.

For the cynichrodene analogs, the 2- and 5-positions are more responsive to electron-withdrawing substituents by resonance than the 3- and 4-positions, whereas negative Δ values were observed for $CpW(CO)_3(CH_3)$, Cp_2Fe, and $CpCo(CO)_2$ derivatives. For $CpMo(CO)_3(CH_3)$ analogs, both negative and positive Δ values were

Table 2
1H NMR data of **1**–**9**.

Compound		Cp(M) (M = Cr or Fe)			
		δ (ppm) H(2,5)	H(3,4)	**Δr**[a]	Others
1	$(CO)_2(NO)CrCp$	5.07	5.07		
	$(CO)_2(NO)Cr(\eta^5\text{-}C_5H_4COOCH_3)$	**5.76**	5.11	0.65	3.80 (OCH_3)
	$(CO)_2(NO)MoCp$	5.59	5.59		3.78 (OCH_3)
2	$(CO)_2(NO)Mo(\eta^5\text{-}C_5H_4COOCH_3)$	**6.23**	5.61	0.62	
	$(CO)_3(CH_3)MoCp$	5.30	5.30		
3	$(CO)_3(CH_3)Mo(\eta^5\text{-}C_5H_4CHO)$	**5.70**	5.51	0.19	0.44 ($Mo(CH_3)$), 9.63 (OCH_3)
4	$(CO)_3(CH_3)Mo(\eta^5\text{-}C_5H_4COCH_3)$	**5.66**	5.43	0.23	0.41 ($Mo(CH_3)$), 2.31 ($-COCH_3$)
5	$(CO)_3(CH_3)Mo(\eta^5\text{-}C_5H_4COOCH_3)$	**5.75**	5.37	0.38	0.44 ($Mo(CH_3)$), 3.81 ($-OCH_3$)
6	$(CO)_3(CH_3)Mo(\eta^5\text{-}C_5H_4\{CH{=}NNH[2,4\text{-}(NO_2)_2C_6H_3]\})$	**5.70**	5.43	0.27	0.45 ($Mo(CH_3)$), 7.92 (Ph, H(6)), 8.35 (Ph, H(5)), 9.15 (Ph, H(3)), 7.82 (−CH=N), 11.24 (NH)
7	$CO)_3(CH_3)Mo(\eta^5\text{-}C_5H_4\{C(CH_3){=}NNH[2,4\text{-}(NO_2)_2C_6H_3]\})$	**6.12**	5.71	0.41	0.32 ($Mo(CH_3)$), 2.21 ($C(CH_3)$=N), 7.96 (Ph, H(6)), 8.26 (Ph, H(5)), 8.85 (Ph, H(3)), 11.0 (NH)
8	$((CO)_3(CH_3)Mo\{\eta^5\text{-}C_5H_4[C(CH_3){=}N)_2$	**5.72**	5.36	0.36	0.41 ($Mo(CH_3)$), 2.06 ($C(CH_3)$=N)
9	$(CO)_2(NO)Cr(\eta^5\text{-}C_5H_4COC_5H_4)FeCp$[b,c]	**5.82**	5.15	0.67	4.23 (Cp^2(Fe))
	$(CO)_2(NO)Cr(\eta^5\text{-}C_5H_4COC_5H_4)FeCp$[b,d]	**4.83**	4.54	0.29	

[a] **Δr** = δ[H(2,5)] − δ[H(3,4)]. (+: H(2.5)downfield, H(3,4) upfield; −: H(2,5) upfield, H(3,4) downfield). The lower-field chemical shift of each pair is indicated in bold.
[b] From Ref. [7].
[c] Cp(M) = Cp(Cr).
[d] Cp(M) = Cp(Fe).

observed (−3.12 for **3**, −1.82 for **4**, and 0.35 for **5**). The largest negative Δ values observed for Cp(Co) derivatives correlated well with the data observed in Table 4b. The carbonyl group withdraws the π electrons from Cp(Co) (Δ3 = 13.07) more readily than from any other Cp(M) derivatives, and least readily from Cp(Cr)(Δ3 = 5.58). The order of the downfield shifts of C(3,4) was consistent with the capability of electron withdrawing by resonance among the following C=O derivatives [12]:

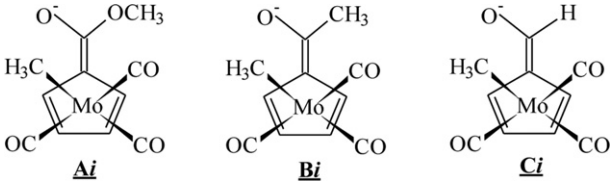

Table 3
$^{13}C\{^1H\}$ NMR data of **1**–**9**.

Compound		Cp(Mo) or Cp(Cr) δ (ppm)				−C(O)−	Mo(CO) or Cr(CO)	$M(CH_3)$	Others
		C(1)	C(2,5)	C(3,4)	**Δr**[a] (ppm)				
1	$(CO)_2(NO)CrCp$	90.31	90.31	90.31	0		237.10		
	$(CO)_2(NO)Cr(\eta^5\text{-}C_5H_4COOCH_3)$	92.94	**94.12**	91.74	2.38	165.07	234.67		52.16(OCH_3)
	$(CO)_2(NO)MoCp$	93.43	93.43	93.43	0		226.90		
2	$(CO)_2(NO)Mo(\eta^5\text{-}C_5H_4COOCH_3)$	97.56	**97.05**	95.05	2.00	164.22	224.55		52.10(OCH_3)
	$(CO)_3(CH_3)MoCp$	92.44	92.44	92.44	0		226.76, 239.89	−22.29	
3	$(CO)_3(CH_3)Mo(\eta^5\text{-}C_5H_4CHO)$	104.15	93.01	**96.13**	−3.1	185.47	223.70, 235.94	−19.64	
4	$(CO)_3(CH_3)Mo(\eta^5\text{-}C_5H_4COCH_3)$	104.72	93.32	**95.14**	−1.8	193.63	224.51, 236.82	−19.41	26.45($CO\underline{C}H_3$)
5	$(CO)_3(CH_3)Mo(\eta^5\text{-}C_5H_4COOCH_3)$	97.80	**94.41**	94.06	0.35	164.83	224.79, 237.42	−19.58	52.08(OCH_3)
6	$(CO)_3(CH_3)Mo(\eta^5\text{-}C_5H_4\{CH{=}NNH[2,4\text{-}(NO_2)_2C_6H_3]\})$	105.40	92.30	**93.47**	−1.20		226.48, 239.42	−18.66	116.28(C(6), Ph), 122.49(C(3)), 129.15(C(2)), 129.25(C(5)), 136.69(C(4)), 143.03(CH=N), 143.78(C(1))
7	$(CO)_3(CH_3)Mo(\eta^5\text{-}C_5H_4\{C(CH_3){=}NNH[2,4\text{-}(NO_2)_2C_6H_3]\})$	114.40	92.76	**94.13**	−1.40		227.29, 240.07	−18.66	13.48 (C(CH3))116.87(C(6), Ph), 123.46(C(3)), 130.52(C(2)), 131.18(C(5)), 139.22(C(4)), 145.37(C(1)), 148.25(C=N)
8	$(CO)_3(CH_3)Mo\{\eta^5\text{-}C_5H_4[C(CH_3){=}N{-}N{=}C(CH_3)](\eta^5\text{-}C_5H_4)\}Mo(CO)_3(CH_3)$	109.50	91.75	**92.60**	−0.8		225.99, 238.73	−19.07	15.23($-C\underline{C}H_3$)), 155.09(−C=N−)
9	$(CO)_2(NO)Cr(\eta^5\text{-}C_5H_4COC_5H_4)FeCp$[b,c]	103.03	**93.89**	91.06	2.83				
	$(CO)_2(NO)Cr(\eta^5\text{-}C_5H_4COC_5H_4)FeCp$[b,d]	78.39	70.43	**72.25**	−1.82				

[a] Δ = δ[C(2,5)] − δ[C(3,4)] (+: C(2.5)downfield, C(3,4) upfield; −: C(2,5) upfield, C(3,4) downfield). The lower-field chemical shift of each pair is indicated in bold.
[b] From Ref. [7].
[c] Cp(M) = Cp(Cr).
[d] Cp(M) = Cp(Fe).

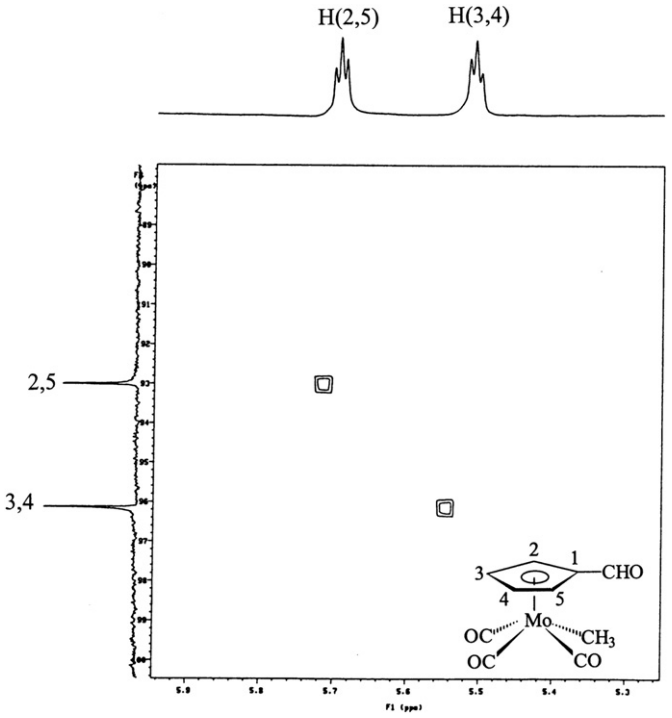

Fig. 2. 2D $^{1}H\{^{13}C\}$ HetCOR NMR spectrum of **3** in $CDCl_3$.

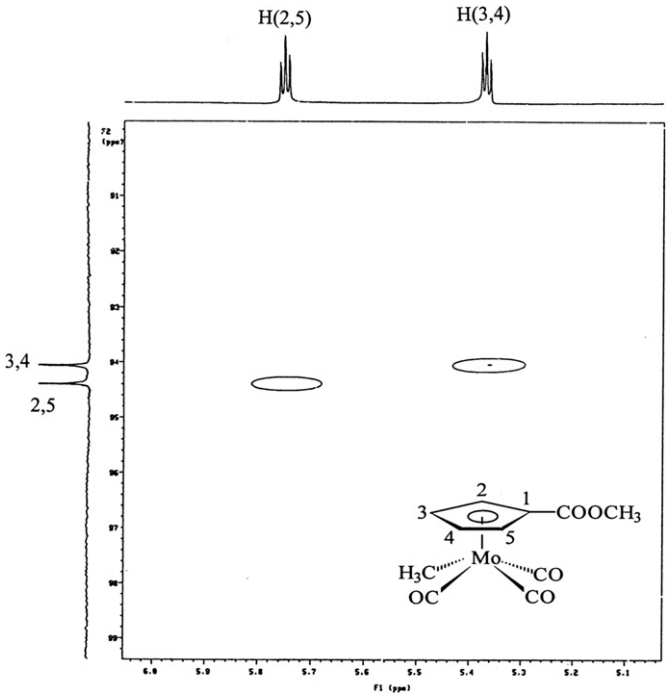

Fig. 3. 2D $^{1}H\{^{13}C\}$ HetCOR NMR spectrum of **5** in $CDCl_3$.

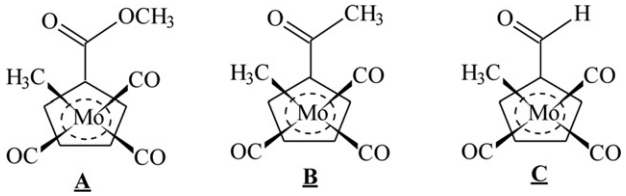

The resonance between the carbonyl and the methoxy oxygen diminishes the extent of the contribution of **A***i* to **A**. Two factors might account for the trend observed between the aldehyde and ketone. First, the electron-donating property of the $-CH_3$ group weakens the electron-withdrawing

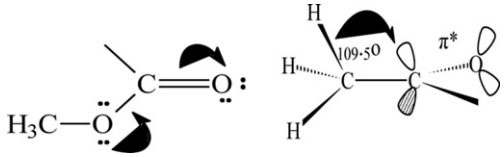

capability of C═O. Second, the hyperconjugation [18] between $-CH_3$ and the carbonyl group diminishes the extent of the contribution of **B***i* to **B**. Compared to the resonance exerted in **C**, the more effective resonance between the carbonyl and the methoxy oxygen or the methyl group diminishes the extent of the resonance between the carbonyl and Cp(Co) in **A** or **B**, respectively. This leads to a greater contribution of **C***i* than **B***i* or **A***i* to each of the corresponding structures **C**, **B** or **A**, and larger negative Δ values in all selected aldehyde derivatives. Conversely, the smallest negative Δ values in all selected ester derivatives were observed (Table 4a).

The trends observed in Table 4a correlate well with the data shown in Table 5: $(CO)_2(NO)Cr(C_5H_4R)$ $(0.51 < 0.56 < 0.65)$; C_6H_5R $(0.27 < 0.41 < 0.56)$; $(CO)_3(CH_3)Mo(C_5H_4R)$ $(0.20 < 0.26 < 0.39)$; $(CO)_3(CH_3)W(C_5H_4R)$ $(0.13 < 0.18 < 0.33)$; $CpFe(C_5H_4R)$ $(0.19 < 0.30 < 0.40)$; and $(CO)_2Co(C_5H_4R)$ $(-0.06 < 0.07 > 0.13)$: $-CHO > -COCH_3 > -COOCH_3$. Here, electron withdrawing by induction deshields the H(2,5), whereas electron withdrawing through resonance deshields the H(3,4). As the effects become competitive, the value of Δ diminishes.

3.2. π-Electron shortage in Cp(Cr) versus π-electron richness in Cp(Co)

From Table 4b, another interesting feature is revealed: the organic carbonyl withdraws the Cp(M) electrons via both induction and resonance. Electron withdrawing by induction predominantly acts on the Cp(Cr) of $(CO)_2(NO)CrCp$ (10.28) derivatives. Electron withdrawing by resonance predominantly, and most prominently, acts on the Cp(Co) of $(CO)_2CoCp$(13.07) derivatives.

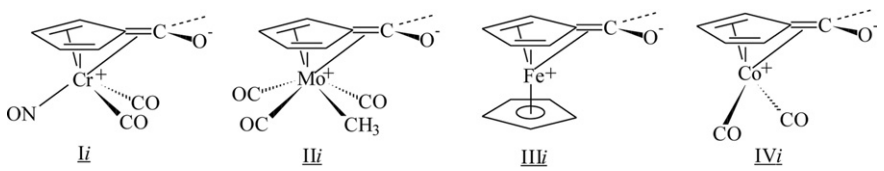

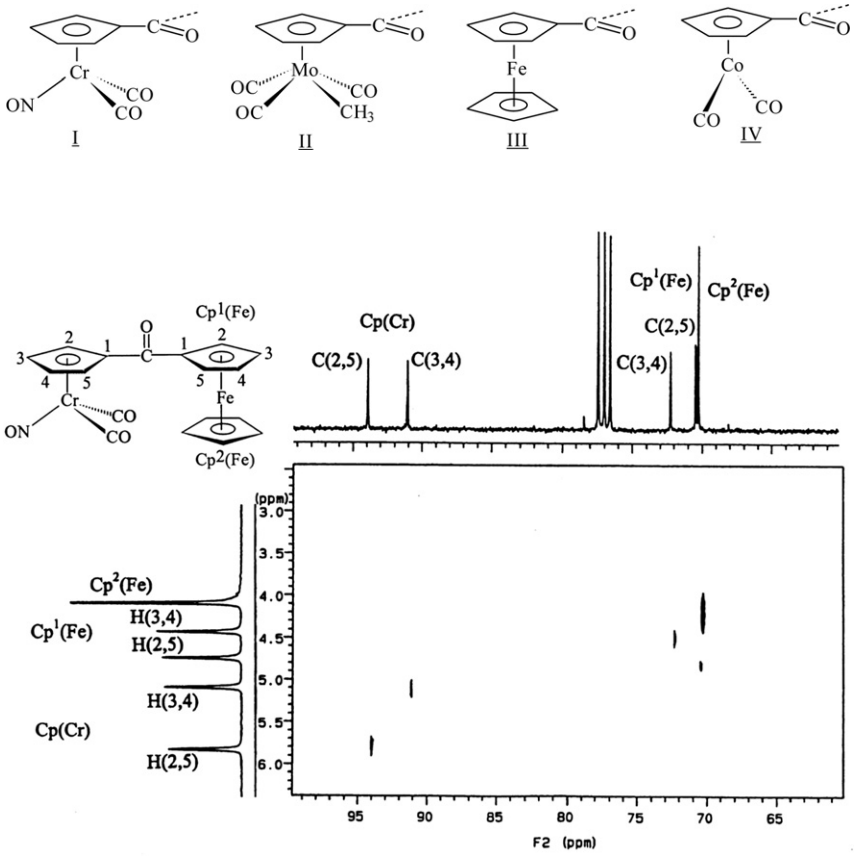

Fig. 4. 2D $^{1}H\{^{13}C\}$ HetCOR NMR spectrum of **9** in $CDCl_3$.

The results demonstrate that the extent of the contribution of the canonical forms **I***i*–**IV***i* to each corresponding structure **I**–**IV** follows in the order **I***i* < **III**, **III***i* < **IV***i*. This trend is plausible [15]. Indeed, as the metal was coordinated with strong electron-withdrawing ligands, the cation was destabilized and the extent of the contribution of the canonical form *i* to the corresponding structure diminished. Conversely, for metals coordinated with weaker or less electron-withdrawing ligands, the extent of the contribution of the canonical form *i* to the corresponding structure increases. In the case of $(CO)_2(NO)CrCp$ derivatives, the overall electron-withdrawing properties of two CO and one NO ligands destabilize the chromium cation, which may lead **I***i* to an insignificant weight of contribution to **I**. The electron withdrawing by induction, deshielding the nearby carbon (C(2,5)) atoms to a greater extent than the more distant 3- and 4-positions, may explain the observed data for $(CO)_2(NO)CrCp$ derivatives. For $(CO)_2CoCp$ derivatives, the canonical form *i* may contribute significantly to each corresponding structure. The electron-withdrawing effect by resonance, acting predominantly on C(3,4) and deshielding the C(3,4), may explain the observed data.

3.3. $(CO)_3(CH_3)Mo(C_5H_4CHO)$ **3** versus $(CO)_3(CH_3)Mo(C_5H_4COOCH_3)$ **5**

It is interesting to compare the ^{13}C chemical shifts of C(2,5) and C(3,4) of Cp(Mo) in the cases of **3** and **5**. Based on the fact that the greater the richness of the π-electron in Cp(M), the greater the extent of the contribution of the canonical form *i* to the corresponding compound, and the formyl group withdraws the π electrons from Cp(M) more readily than does the ester group. In

Table 4a
^{13}C NMR chemical shifts in the ring of selected monosubstituted $(CO)_2(NO)CrCp$[a], $(CO)_3(CH_3)MoCp$[b], $(CO)_3(CH_3)WCp$[c], Cp_2Fe[d], and $(CO)_2CoCp$[e] derivatives.

R=	$(CO)_2(NO)Cr(C_5H_4R)$			$(CO)_3(CH_3)Mo(C_5H_4R)$			$(CO)_3(CH_3)W(C_5H_4R)$			$CpFe(C_5H_4R)$			$(CO)_2Co(C_5H_4R)$		
	δ (ppm)		**Δr**[f]	δ (ppm)		**Δr**	δ (ppm)		**Δr**	δ (ppm)		**Δr**	δ (ppm)		**Δr** (ppm)
	C(2,5)	C(3,4)		C(2,5)	C(3,4)		C(2,5)	C(3,4)		C(2,5)	C(3,4)		C(2,5)	C(3,4)	
−CHO	**93.53**	92.76	0.77	93.01	**96.13**	−3.12	91.16	**95.17**	−4.01	68.0	**72.6**	−4.6	83.44	**89.47**	−6.03
$-COCH_3$	**93.56**	92.01	1.55	93.32	**95.14**	−1.82	91.60	**94.19**	−2.59	69.2	**71.8**	−2.6	83.58	**88.33**	−4.75
$-COOCH_3$	**94.12**	91.74	2.38	**94.41**	94.06	0.35	92.89	**93.17**	−0.28	69.8	**71.0**	−1.2	86.06	**88.86**	−2.80

[a] From Refs. [13,14].
[b] From [this work].
[c] From [this work, [15]].
[d] From Refs. [16,17].
[e] [This work].
[f] **Δr** = δ[C(2,5)] − δ[C(3,4)], (+: C(2.5)downfield, C(3,4) upfield; −: C(2,5) upfield, C(3,4) downfield). The lower-field chemical shift of each pair is indicated in bold.

Table 4b
A comparison of the relative ^{13}C NMR chemical shifts in the ring of selected monosubstituted $(CO)_2(NO)CrCp$, $(CO)_3(CH_3)WCp$, Cp_2Fe and $(CO)_2CoCp$ derivatives.

R=	$(CO)_2(NO)Cr(C_5H_4-R)$			$(CO)_3(CH_3)Mo(C_5H_4-R)$			$(CO)_3(CH_3)W(C_5H_4-R)$			$CpFe(C_5H_4-R)$			$(CO)_2Co(C_5H_4-R)$		
	^{13}C (ppm, from δ 90.31[a])			^{13}C (from δ 92.44[a])			^{13}C (from δ 91.18[a])			^{13}C (from δ 67.88[a])			^{13}C (from δ 84.51[a])		
	Δ^1	Δ^2	Δ^3	Δ^1	Δ^2	Δ^3	Δ^1	Δ^2	Δ^3	Δ^1	Δ^2	Δ^3	Δ^1	Δ^2	Δ^3
	C(1)	C(2,5)	C(3,4)	C(1)	C(2,5)	C(3,4)	C(1)	C(2,5)	C(3,4)	C(1)	C(2,5)	C(3,4)	C(1)	C(2,5)	C(3,4)
−CHO	9.97	3.22	2.45	11.71	0.57	3.69	10.83	−0.02	3.99	11.32	0.12	4.72	16.04	−1.07	4.96
$-COCH_3$	10.55	3.25	1.7	12.28	0.88	2.7	11.42	0.42	3.01	11.42	1.32	3.92	15.71	−0.93	3.82
$-COOCH_3$	2.63	3.81	1.43	5.36	1.97	1.62	4.46	1.71	1.99	8.14	1.92	3.13	8.3	1.5	4.35
Sum[b]		10.28	5.58		3.42	8.01		2.11	8.99		3.36	11.77		−0.45	13.07

$\Delta^1 = \delta$ C(1) − δ (parent compound). $\Delta^2 = \delta$ C(2,5) − δ (parent compound). $\Delta^3 = \delta$ C(3,4) − δ (parent compound).
[a] Chemical shifts of corresponding parent compound (R = H).
[b] Sum of the values corresponding to −CHO, $-COCH_3$ and $-COOCH_3$.

a compound bearing both −CHO and electron-rich Cp(M), as in the case of $(CO)_2Co(C_5H_4CHO)$, positions 3 and 4 on the substituted Cp ring would be anticipated to be more sensitive to electron-withdrawing substituents. However, a compound bearing both $-COOCH_3$ and electron-depleted Cp(M), as in the case of $(CO)_2(NO)Cr(C_5H_4COOCH_3)$, positions 2 and 5 on the substituted Cp ring would be anticipated to be more sensitive to electron withdrawing.

One may wonder whether for a compound like **3** or **5**, in which the π-electron of Cp(M) is caught in the middle of electron richness and electron poorness, the assignments of chemical shifts, downfield or upfield, for C(2,5) and C(3,4) of Cp(Mo) will follow the ferrocene or the cynichrodene analogs. The finding that complex **3** exhibits a negative slope whereas **5** exhibits a positive slope, seems initially counterintuitive. To the best of our knowledge, this is the first published report that among the same Cp(M) analogs, the C(3,4) and the C(2,5) are inversely assigned to downfield shifts for Cp(M) bearing different carbonyl electron-withdrawing substituents. The result is plausible, as mentioned earlier, that the formyl group withdraws the π electrons from Cp(M) more readily than does the ester group, so the compound **3** would be anticipated to follow the assignments of the ferrocene analog, whereas **5** would be anticipated to follow the assignments of the cynichrodene analog.

3.4. X-ray: similarity between metallocenyl carbocation and π-electron enriched Cp(M) bearing carbonyl group

The molecular structures of **7** and **8** are shown in Figs. 5 and 6. Selected bond distances and angles are given in Tables 7 and 8. The methyl ligand is located at the site toward the exocyclic organic carbonyl carbon with twist angles of 69.1° and 60.4°, respectively. The twist angle is defined as the torsional angle between the methyl carbon atom, the Mo atom, the Cp ring center and the ring C atom bearing the exocyclic carbon.

Table 9 lists selected structural data of the series of some organometallic Cp(M) complexes bearing an electron-withdrawing carbonyl group—$(CO)_2(NO)Cr(C_5H_4CHO)$ [19], $(CO)_3(CH_3)Mo(C_5H_4COCH_3)$ **4** [20], $(CO)_3(CH_3)W(\eta^5\text{-}C_5H_4COCH_3)$ [20], $CpFe(C_5H_4COCH_3)$ [21], $CpFe(C_5H_4COCH_3)$ [22], and $(CO)_2Co(\eta^5\text{-}C_5H_4COONS)$ **11** [23].

Several important features are observed. The exocyclic carbon is bending toward or only slightly bent away from the metal atom with a positive, or a small negative, value of the angle θ. Presumably, a higher negative θ value would be anticipated if the steric strain between the Cp-substituent and the M-coordinated ligands was considered, as for complex **10** (−4.69°) [24]. The θ angle is defined as the angle between the exocyclic C–C bond (C1–C6) and the corresponding Cp ring with a positive angle when bending toward the metal and a negative angle when bending away from the metal. Both the exocyclic C–C bond of the Cp(M) ring and the length of the metal–C(exocyclic) bond in these Cp(M) complexes are considerably shorter than those of **10** (1.497(9) Å and 3.456(9) Å). Furthermore, they all reveal either a long–short–short–short–long or a long–short–long–short–long pattern of the carbon–carbon bond lengths in the Cp(M) ring.

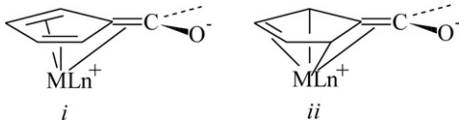

i *ii*

The above observations—(1) a positive or a small negative value of θ, (2) a short exocyclic C–C bond of the Cp(M) ring, (3) a short M–C(exocyclic) distance, and (4) a long–short–short–short–long or a long–short–long–short–long pattern of carbon–carbon bond lengths in the Cp(M)—may be explained by the contribution of the canonical forms *i* (a L_2 form) or *ii* (a LX_2 form) to each corresponding compound.

From Table 9, we observed that the ruthenocenylmethylium cation **14** [25] also exhibits the characteristics listed above. The resemblance between the two canonical forms (*i* and **14***i*) of these two categories may explain the observation.

Table 5
^1H NMR chemical shifts of selected monosubstituted $(CO)_2(NO)CrCp$, C_6H_6, $(CO)_3(CH_3)MoCp$, $(CO)_3(CH_3)WCp$, Cp_2Fe, and $(CO)_2CoCp$ derivatives from tetramethylsilande and Δ.[a]

R=	$(CO)_2(NO)Cr(CpR)$			C_6H_5R			$(CO)_3(CH_3)Mo(C_5H_4R)$			$(CO)_3(CH_3)W(CpR)$			$(C_5H_5)Fe(C_5H_4R)$			$(CO)_2Co(C_5H_4-R)$		
	δ (ppm)		Δ	δ (ppm)		Δ	δ (ppm)		Δ	δ (ppm)		Δ	δ (ppm)		Δ	δ (ppm)		Δ
	H(2,5)	H(3,4)		H(2)	H(4)		H(2,5)	H(3,4)		H(2,5)	H(3,4)		H(2,5)	H(3,4)		H(2,5)	H(3,4)	
−CHO	5.75	5.24	0.51	7.81	7.54	0.27	5.72	5.52	0.20	5.72	5.59	0.13	4.79	4.60	0.19	5.38	5.44	−0.06
$-COCH_3$	5.72	5.16	0.56	7.86	7.45	0.41	5.73	5.47	0.26	5.71	5.53	0.18	4.66	4.36	0.30	5.40	5.33	0.07
$-COOCH_3$	5.76	5.11	0.65	8.01	7.45	0.56	5.78	5.39	0.39	5.79	5.46	0.33	4.80	4.40	0.40	5.65	5.50	0.15
			1.72			1.24			0.80			0.64			0.89			0.16

[a] $\Delta = \delta$[H(2)] − δ[H(4)] for benzene derivatives; $\Delta = \delta$[H(2,5)] − δ[H(3,4)] for $(CO)_2(NO)CrCp$, Cp_2Fe, $(CO)_3(CH_3)MoCp$, $(CO)_3(CH_3)WCp$ and $(CO)_2CoCp$ derivatives. (+: H(2.5) downfield, H(3,4) upfield; −: H(2,5) upfield, H(3,4) downfield).

Table 6
The contracted 2D HetCOR spectra of −CHO, $-COCH_3$, $-COOCH_3$ derivatives of $(CO)_2(NO)CrCp$, $(CO)_3(CH_3)MoCp$, $(CO)_3(CH_3)WCp$, Cp_2Fe, and $(CO)_2CoCp$.

Compound	R=	Cp(M)	^{1}H, Cp(M)[a]	2D HetCOR[b]	^{13}C, Cp(M)[a]
$(CO)_2(NO)Cr(\eta^5\text{-}C_5H_4R)$	CHO, $COCH_3$, $COOCH_3$	Cp(Cr)			
$(CO)_3(CH_3)Mo(\eta^5\text{-}C_5H_4R)$	$COOCH_3$	Cp(Mo)			
$(CO)_3(CH_3)Mo(\eta^5\text{-}C_5H_4R)$	CHO, $COCH_3$	Cp(Mo)			
$(CO)_3(CH_3)W(\eta^5\text{-}C_5H_4R)$	CHO, $COCH_3$, $COOCH_3$	Cp(W)			
$CpFe(\eta^5\text{-}C_5H_4R)$	CHO, $COCH_3$, $COOCH_3$	Cp(Fe)			
$(CO)_3(CH_3)Co(\eta^5\text{-}C_5H_4R)$	$COCH_3$, $COOCH_3$	Cp(Co)			
$(CO)_3(CH_3)Co(\eta^5\text{-}C_5H_4R)$	CHO	Cp(Co)			

[a] ∘, (2,5); *, (3,4); the magnetic field increases toward the right.
[b] The magnetic fields of ^{1}H and ^{13}C NMR spectra increase toward the right and upper side respectively.

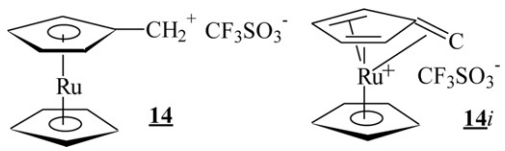

3.5. C(3,4) of Cp(M) deshielded by EW carbonyl groups

From the obtained chemical shifts of Cp(M), observed or literature-reported, it was consistently revealed that for those organometallic complexes with π-electron enriched Cp(M), as ferrocene analogs [12], C(3,4) are more sensitive to electron-withdrawing carbonyl substituents.

One may wonder what is the reason why the electron-withdrawing carbonyl groups—CHO, $COCH_3$, and $COOCH_3$—deshield the C(3,4) to a greater extent than the C(2,5). The resemblance between the canonical forms of carbocation **14** and those of Cp(M) analog bearing electron-withdrawing carbonyl substituents, aroused our curiosity to compare the chemical shifts of ^{13}C NMR between these two categories. Amazingly, an excellent correlation was observed.

Table 10 [25,26] listed the selected ^{13}C NMR data of carbocations **12**–**14**. Compared to the data listed in Table 3, it is worth noting that the C(3,4) resonate at a much lower field than C(2,5), and relatively large negative values of $\Delta\mathbf{r}$ (−13.2 ppm for **12**, −8.29 ppm for **13**, −6.00 ppm for **14**) were observed in all three cases. These results may adequately indicate that C(3,4) are more deshielded than C(2,5) in ferrocene analogs bearing electron-withdrawing carbonyl substituents. The correlation therefore indicates that the change in the magnitude of the bending of the exocyclic carbon toward the metal of Cp(M) is proportional to the change in the extent of deshielding on C(3,4) of Cp(M). However, for bulky ligands or a comparison between Cp rings with different numbers of the legs of the piano stool Cp-complexes, the relationship may fail because

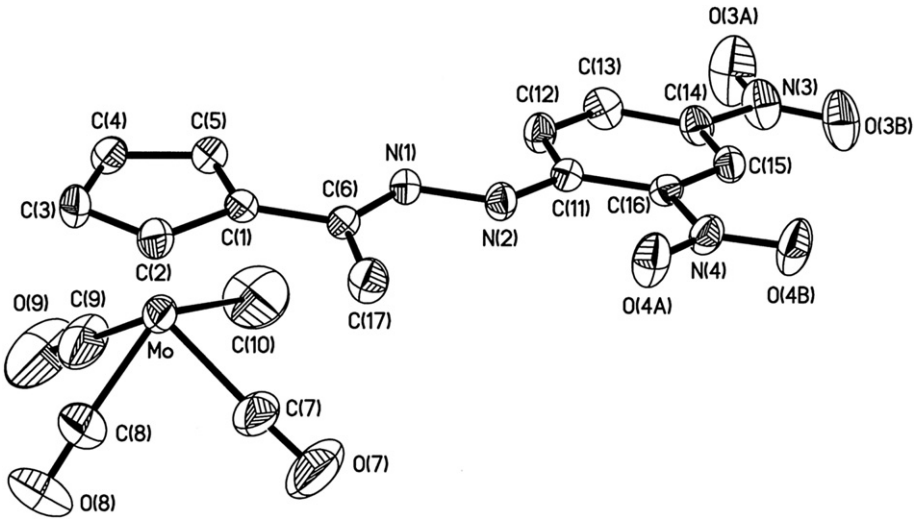

Fig. 5. Molecular configuration of **7**.

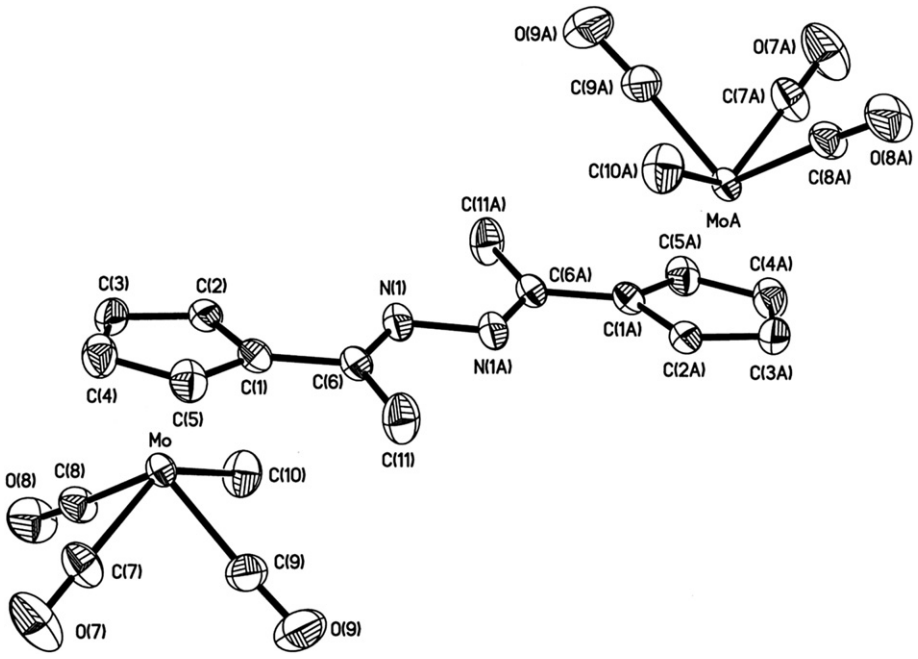

Fig. 6. Molecular configuration of **8**.

Table 7
Selected bond length (Å) and selected bond angles (°) for **7**.

Mo–C(1)	2.343(4)	C(6)–C(1)–C(2)	127.4(4)
Mo–C(2)	2.306(5)	C(6)–C(1)–C(5)	126.5(3)
Mo–C(3)	2.309(5)	C(1)–C(6)–N(1)	115.3(3)
Mo–C(4)	2.351(4)	C(7)–Mo–C(8)	78.1(3)
Mo–C(5)	2.352(4)	C(7)–Mo–C(9)	106.7(3)
C(1)–C(2)	1.419(5)	C(7)–Mo–C(10)	72.1(3)
C(1)–C(5)	1.411(6)	Mo–C(7)–O(7)	177.1(6)
C(1)–C(6)	1.463(5)	Mo–C(8)–O(8)	177.2(8)
C(2)–C(3)	1.402(6)	Mo–C(9)–O(9)	177.0(8)
C(3)–C(4)	1.386(7)	C(6)–N(1)–N(2)	115.9(3)
C(4)–C(5)	1.403(6)	Cp(cen.)–Mo–C(7)	125.82
C(6)–C(17)	1.495(6)	Cp(cen.)–Mo–C(8)	118.61
Mo–C(7)	1.960(6)	Cp(cen.)–Mo–C(9)	126.61
Mo–C(8)	1.989(8)	Cp(cen.)–Mo–C(10)	108.90
Mo–C(9)	1.951(7)	C(17)–C(6)–N(1)	125.3(4)
Mo–C(10)	2.281(8)	C(1)–C(6)–C(17)	119.4(3)
C(6)–N(1)	1.287(5)	N(1)–N(2)–C(11)	120.3(3)
C(7)–O(7)	1.133(7)	N(2)–C(11)–C(12)	120.8(3)
C(8)–O(8)	1.121(8)	N(2)–C(11)–C(16)	122.2(3)
C(9)–O(9)	1.148(8)	C(14)–N(3)–O(3A)	117.7(4)
N(1)–N(2)	1.372(4)	C(14)–N(3)–O(3B)	119.4(4)
C(11)–C(12)	1.407(5)	C(16)–N(4)–O(4A)	119.1(3)
C(11)–C(16)	1.419(5)	C(16)–N(4)–O(4B)	119.0(3)
C(11)–N(2)	1.342(5)	N(3)–C(14)–C(13)	120.4(4)
C(12)–C(13)	1.365(6)	N(3)–C(14)–C(15)	117.9(4)
C(13)–C(14)	1.399(6)	N(4)–C(16)–C(11)	122.2(3)
C(14)–C(15)	1.357(6)	N(4)–C(16)–C(15)	116.2(3)
C(15)–C(16)	1.379(5)		
C(14)–N(3)	1.454(5)		
N(3)–O(3A)	1.213(5)		
N(3)–O(3B)	1.208(5)		
C(16)–N(4)	1.439(5)		
N(4)–O(4A)	1.229(4)		
N(4)–O(4B)	1.212(4)		
Mo···Cp(cen.)	2.003		
Dihedral angles between planes			
Cp(cen.), Mo, C(7) and Cp(cen.), Mo, C(1)			12.74
Cp(cen.), Mo, C(8) and Cp(cen.), Mo, C(1)			108.82
Cp(cen.), Mo, C(9) and Cp(cen.), Mo, C(1)			155.00
Cp(cen.), Mo, C(10) and Cp(cen.), Mo, C(1)			69.14
Cp(Mo) and hydrazone plane (C6, N1, N2)		1.26	
Phenyl and hydrazone plane (C6, N1, N2)		6.18	
Cp(Mo) and phenyl		7.38	

Table 8
Selected bond length (Å) and selected bond angles (°) for **8**.

Mo–C(1)	2.322(4)	C(6)–C(1)–C(2)	124.7(4)
Mo–C(2)	2.368(5)	C(6)–C(1)–C(5)	127.9(5)
Mo–C(3)	2.362(5)	C(1)–C(6)–C(11)	118.4(4)
Mo–C(4)	2.317(5)	C(7)–Mo–C(8)	78.6(2)
Mo–C(5)	2.300(4)	C(7)–Mo–C(9)	78.5(3)
C(1)–C(2)	1.438(7)	C(7)–Mo–C(10)	132.4(2)
C(1)–C(5)	1.413(7)	Mo–C(7)–O(7)	178.9(6)
C(1)–C(6)	1.471(6)	Mo–C(8)–O(8)	177.3(5)
C(2)–C(3)	1.414(7)	Mo–C(9)–O(10)	176.9(5)
C(3)–C(4)	1.385(9)	C(1)–C(6)–N(1)	115.8(4)
C(4)–C(5)	1.412(7)	C(11)–C(6)–N(1)	125.8(4)
C(6)–C(11)	1.487(7)	C(6)–N(1)–N(1A)	113.8(5)
Mo–C(7)	1.989(5)	Cr(cen.)–Mo–C(7)	117.70
Mo–C(8)	1.995(5)	Cr(cen.)–Mo–C(8)	126.30
Mo–C(9)	1.962(6)	Cr(cen.)–Mo–C(9)	127.35
Mo–C(10)	2.299(5)	Cr(cen.)–Mo–C(10)	109.92
C(7)–O(7)	1.139(7)	C(8)–Mo–C(9)	105.4(2)
C(8)–O(8)	1.122(6)	C(8)–Mo–C(10)	73.2(2)
C(9)–O(9)	1.152(7)	C(9)–Mo–C(10)	73.3(2)
C(6)–N(1)	1.273(6)		
N(1)–N(1A)	1.410(7)		
Mo···Cp(cen.)	2.001		
Dihedral angles between planes			
Cp(cen.), Mo, C(7) and Cp(cen.), Mo, C(1)			120.06
Cp(cen.), Mo, C(8) and Cp(cen.), Mo, C(1)			147.30
Cp(cen.), Mo, C(9) and Cp(cen.), Mo, C(1)			23.38
Cp(cen.), Mo, C(10) and Cp(cen.), Mo, C(1)			60.37
Cp(Mo) and azine plane (C6, N1, N1A, C6A)			10.17
Cp(MoA) and azine plane (C6, N1, N1A, C6A)			10.15
Cp(Mo) and Cp(MoA)			0.06

of the different extent of steric effects. Furthermore, for potential π-acceptor ligands, such as NO in cynichrodene analogs, the extent of bending may be enhanced due to the increased contribution of *i* to the corresponding compound via the electron donating of the exocyclic double bond to the transoid NO ligand.

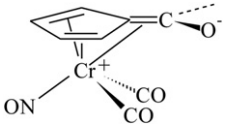

After obtaining the X-ray structures of **4** [20], **7**, and **8**, the average charges of C(2,5) and C(3,4) for complex **4** (−0.4054 and −0.2540), **7** (−0.4318 and −0.3012), and **8** (−0.3998 and −0.2959) were determined by ab-initio calculations (Table 11). These values correlate well with the unequivocal assignments of the ^{13}C chemical shifts (Table 3). The electron density on C(2,5) is higher than that on C(3,4).

4. Conclusion

Several important findings may be drawn as follows and the electronic effects appear to account for all the observations.

Table 9
Selected structural data.

Compound	M	Bond length (Å)	M–C(exocyclic)								
		C(Cp(M))–C(exocyclic)	ωM (°)[a]		θM (°)[b]		Cp(M)				
							C1–C2	C2–C3	C3–C4	C4–C5	C1–C5
$(CO)_2(NO)Cr(\eta^5\text{-}C_5H_4CHO)$[c]	Cr	1.470(8)	NO	175.3	1.53	3.207	1.427(7)	1.406(7)	1.423(7)	1.410(7)	1.438(6)
4 $(CO)_3(CH_3)Mo(\eta^5\text{-}C_5H_4COCH_3)$[d]	Mo	1.478(5)	CH_3	130.2	−0.57	3.301	1.427(5)	1.403(5)	1.408(5)	1.413(5)	1.424(5)
7 $(CO)_3(CH_3)Mo(\eta^5\text{-}C_5H_4C(CH_3)=NNHR)$[e]	Mo	1.463(5)	CH_3	69.1	−0.19	3.347	1.419(5)	1.402(6)	1.386(7)	1.403(6)	1.411(6)
$(CO)_3(CH_3)W(\eta^5\text{-}C_5H_4COCH_3)$[d]	W	1.471(9)	CH_3	58.8	−0.44	3.298	1.426(9)	1.385(11)	1.409(11)	1.396(10)	1.426(9)
10 $[(CO)_3W(\eta^5\text{-}C_5H_4(CH_2)_3\text{–}\eta^1\text{-}CH_2)]$[f]	W	1.497(9)	CH_2	32.5	−4.69	3.456	1.431(9)	1.412(9)	1.417(9)	1.417(9)	1.421(9)
$CpFe(\eta^5\text{-}C_5H_4CHO)$[g]	Fe	1.445(5)			4.90	3.004	1.401(6)	1.390(6)	1.404(7)	1.350(6)	1.384(6)
$CpFe(\eta^5\text{-}C_5H_4COCH_3)$[h]	Fe	1.493(5)			2.16	3.116	1.436(6)	1.410(6)	1.407(7)	1.418(6)	1.431(6)
11 $(CO)_2Co(\eta^5\text{-}C_5H_4COONS)$[i]	Co	1.438(7)			2.61	3.090	1.435(7)	1.395(8)	1.384(8)	1.423(8)	1.413(7)
14 $CpRu(\eta^5\text{-}C_5H_4CH_2^+)(CF_3SO_3^-)$[j]	Ru	1.405(6)			42.6	2.272	1.458(6)	1.413(7)	1.429(6)	1.412(6)	1.459(6)

[a] ωM(°): the twist angle is defined as the torsional angle between chlorine atom (or methyl or methylene carbon), the tungsten atom, the Cp center and the ring carbon atom bearing the exocyclic carbon atom.
[b] θM(°) : the θ angle is defined as the angle between the exocyclic C–C bond and the corresponding Cp ring with a positive angle toward metal and a negative angle away from the metal.
[c] From Ref. [19].
[d] From Ref. [20].
[e] R = 2.4-dinitrophenyl, from [this work].
[f] From Ref. [24].
[g] From Ref. [21].
[h] From Ref. [22].
[i] NS = *N*-succinimidyl, from Ref. [23].
[j] From Ref. [25].

Table 10
Selected $^{13}C\{^1H\}$ NMR data of **12**–**14**.

Compound	M	$Cp^1(M)$ (δ (ppm))			**Δr**[a] (ppm)	C^+	$Cp^2(M)$
		C(1)	C(2,5)	C(3,4)			
12 $(CO)_2(NO)Cr[(\eta^5\text{-}C_5H_4)CH^+(BF_4^-)(\eta^5\text{-}C_5H_4)]FeCp$[b]	Fe	99.09	80.76	**93.96**	−13.2	120.0	83.06
13 $(CO)_2(NO)Cr[(\eta^5\text{-}C_5H_4)CH^+(BF_4^-)(\eta^5\text{-}C_5H_4)]RuCp$[b]	Ru	99.77	83.59	**91.88**	−8.29	94.72	85.37
14 $[CpRu(C_5H_4CH_2)]^+[BAr'_4]^-$[c]	Ru	108.0	86.4	**92.4**	−6.0	72.1	84.1

[a] $\mathbf{\Delta r} = \delta[C(2,5)] - \delta[C(3,4)]$ (+: C(2.5)downfield, C(3,4) upfield; −: C(2,5) upfield, C(3,4) downfield). The lower-field chemical shift of each pair is indicated in bold.
[b] From Ref. [26].
[c] From Ref. [25].

(a) In all the selected Cp(M) derivatives, the capability of deshielding the C(3,4) carbons is arranged in the same order: −CHO > −$COCH_3$ > −$COOCH_3$.
(b) The organic carbonyl withdraws the π-electron deficient Cp(M) electrons via induction predominantly, whereas it withdraws the π-electron enriched Cp(M) electrons via resonance predominantly.
(c) Among the same Cp(Mo) analog: $(CO)_3(CH_3)Mo(CpR)$, the chemical shifts for C(2,5) and C(3,4) of the formyl derivative **3** follow the assignment of the ferrocene analog, whereas those of the ester derivative **5** follow the assignments of the cynichrodene analog.
(d) Some important structural characteristics were observed for both metallocenyl carbocations and Cp(M) derivatives bearing a carbonyl group.
(e) The extent of deshielding on C(3,4) of Cp(M) was correlated well with the magnitude of nonplanarity of Cp-exocyclic carbon to π-accepting substituent in both metallocenyl carbocations and Cp(M) derivatives bearing a carbonyl group.

5. Experimental details

All the syntheses were carried out under nitrogen by the use of Schlenk techniques. Traces of oxygen in the nitrogen were removed with BASF catalyst, and deoxygenated nitrogen was dried over molecular sieves (3 Å) and P_2O_5. Hexane, pentane, benzene, and dichloromethane were dried over calcium hydride and freshly distilled under nitrogen. Diethyl ether was dried over sodium and redistilled under nitrogen from sodium-benzophenone ketyl. All the other solvents were used as commercially obtained. Column chromatography was carried out under nitrogen with Merck Kiesel-gel 60. The silica gel was heated with a heat gun during mixing in a rotary evaporator attached to a vacuum pump for 1 h to remove water and oxygen. The silica gel was then stored under nitrogen until use. ^1H, ^{13}C NMR, and 2D $^1H\{^{13}C\}$ HETCOR (HETeronuclear COrrelation) experiments were acquired on a Varian Unity-300 spectrometer. Chemical shifts were referenced to tetramethylsilane. IR spectra were recorded using a Perkin–Elmer Fourier transform IR 1725X spectrophotometer. Microanalyses were carried out by the Microanalytic Laboratory of the National Chung Hsing University. Complexes **2** [2] and **3**–**5** [3] were prepared by following the published procedures. Their characterizations are given in Tables 2 and 3.

Table 11
Selected net atomic charges for **4**, **7**, and **8** using the LANL2DZ basis set.

	C(1)	C(2)	C(3)	C(4)	C(5)
4	0.283611	−0.424538	−0.224112	−0.283875	−0.386181
7	0.338381	−0.442862	−0.302288	−0.300083	−0.420753
8	0.278151	−0.388977	−0.285833	−0.305908	−0.410621

5.1. Preparation of (η^5-formylcyclopentadienyl) tricarbonylmethylmolybdenum 2,4-dinitrophenylhydrazone **6**

(η^5-Formylcyclopentadienyl)tricarbonylmethylmolybdenum **3** (1.44 g, 5.0 mmol) was dissolved in 50 ml of methanol, and $BF_3\cdot OEt_2$ (0.65 ml, 5.0 mmol) was dropped into it at −78 °C. After stirring for 20 min, 2,4-dinitrophenylhydrazine (1.0 g, 5.0 mmol) was added and the reaction mixture was allowed to stir 3.5 h at room temperature. A dark orange–red solid precipitated. After suction filtration, the precipitate was washed with 10 ml of cold methanol. Compound **6** was obtained as a dark orange–red solid (2.1 g, 90%).

Anal. Found: C, 41.13; H, 2.76; N, 11.92. $C_{16}H_{12}N_4O_7Mo$ Calc.: C, 41.04; H, 2.58; N, 11.97%. Proton NMR ($CDCl_3$): δ (relative intensity, multiplicity, assignment): 0.45 (CH_3); 5.43 (2H, t, $J = 2.4$ Hz, Cp(Mo) H(3,4)); 5.70 (2H, t, $J = 2.4$ Hz, Cp(Mo) H(2,5)); 7.92 (1H, d, $J = 9.6$ Hz, Ph H(6)); 8.35 (1H, d of d, $J = 9.6$ Hz, 2.7 Hz, Ph H(5)); 7.82 (1H, s, −CH═N); 9.15 (1H, d, $J = 2.7$ Hz, Ph H(3)); 11.24 (1H, brs, NH). Carbon-13 NMR ($CDCl_3$): δ (assignment): −18.66 (CH_3); 92.30 (Cp(Mo), C(2,5)); 93.47 (Cp(Mo), C(3,4)); 105.36 (Cp(Mo), C(1)); 116.28 (Ph, C(6)); 122.49 (Ph, C(3)); 129.15 (Ph, C(2)); 129.25 (Ph, C(5)); 136.69 (Ph, C(4)); 143.03 (CH═N); 143.78 (Ph, C(1)); 226.48, 239.42 (Mo–C≡O). IR(KBr): ν (cm^{-1}) (intensity): 2020 (s), 1936(vs), 1622(m), 1591(w), 1511(w), 1337(w). Mass spectrum: m/z: 468 (M^+).

5.2. Preparation of (η^5-acetylcyclopentadienyl) tricarbonylmethylmolybdenum 2,4-dinitrophenylhydrazone **7**

(η^5-Acetylcyclopentadienyl)tricarbonylmethylmolybdenum **4** (1.51 g, 5.0 mmol) was dissolved in 50 ml of methanol, and $BF_3\cdot OEt_2$ (0.65 ml, 5.0 mmol) was dropped into it at −78 °C. After stirring for 20 min, 2,4-dinitrophenylhydrazine (1.0 g, 5.0 mmol) was added and the reaction mixture was allowed to stir 3.5 h at room temperature. A dark orange–red solid precipitated. After suction filtration, the precipitate was washed with 10 ml of cold methanol. Compound **7** was obtained as a dark orange–red solid (2.24 g, 92.9%).

Anal. Found: C, 42.48; H, 2.97; N, 11.48 $C_{17}H_{14}N_4O_7Mo$ Calc.: C, 42.34; H, 2.93; N, 11.62%. Proton NMR ($CDCl_3$): δ (relative intensity, multiplicity, assignment): 0.32 ($MoCH_3$); 2.21 ($C(CH_3)$); 5.71 (2H, t, $J = 2.4$ Hz, Cp(Mo) H(3,4)); 6.12 (2H, t, $J = 2.4$ Hz, Cp(Mo) H(2,5)); 7.96 (1H, d, $J = 9$ Hz, Ph H(6)); 8.26 (1H, d of d, $J = 9$ Hz, 2.4 Hz, Ph H(5)); 8.85 (1H, d, $J = 2.4$ Hz, Ph H(3)); 11.00 (1, s, NH). Carbon-13 NMR ($CDCl_3$): δ (assignment): −18.66 ($MoCH_3$); 13.48 ($C\underline{C}H_3$)) 92.76 (Cp(Mo), C(2,5)); 94.13 (Cp(Mo), C(3,4)); 110.40 (Cp(Mo), C(1)); 116.87 (Ph, C(6)); 123.46 (Ph, C(3)); 130.52 (Ph, C(2)); 131.18 (Ph, C(5)); 139.22 (Ph, C(4)); 145.37 (Ph, C(1)); 148.25 (C═N); 227.29, 240.07 (Mo–C≡O). IR(KBr): ν (cm^{-1}) (intensity): 2019 (s), 1951(vs), 1914(vs), 1615(m), 1584(m), 1510(w), 1325(m). Mass spectrum: m/z: 482(M^+).

5.3. Preparation of (η^5-acetylcyclopentadienyl)tricarbonyl-methylmolybdenum azine ***8***

(η^5-Acetylcyclopentadienyl)tricarbonylmethylmolybdenum **4** (1.56 g, 5.16 mmol) was dissolved in 50 ml of methanol, and $BF_3\cdot OEt_2$

(0.65 ml, 5.0 mmol) was dropped into it at −78 °C. After stirring for 20 min, hydrazine (0.064 g, 2.0 mmol) was added and the reaction mixture was allowed to stir 3 h at room temperature. A yellow solid precipitated. After suction filtration, the precipitate was washed with 10 ml of cold methanol. An analytical sample (2.60 g, 97%) of **8** was prepared by recrystallization using the solvent evaporation method from hexane: dichloromethane (5:1) at 0 °C.

Anal. Found: C, 43.63; H, 3.35; N, 4.73. $C_{22}H_{20}N_2O_6Mo_2$ Calc.: C, 44.02; H, 3.36; N, 4.67%. Proton NMR ($CDCl_3$): δ (relative intensity, multiplicity, assignment): 0.41 ($MoCH_3$); 2.06 (CCH_3); 5.36 (2H, t, $J = 2.4$ Hz, Cp(Mo) H(3,4)); 5.72 (2H, t, $J = 2.4$ Hz, Cp(Mo) H(2,5)). Carbon-13 NMR ($CDCl_3$): δ (assignment): −19.07 ($MoCH_3$); 15.23 ($C(\underline{C}H_3)$); 91.75 (Cp(Mo), C(2,5)); 92.60 (Cp(Mo), C(3,4)); 109.53 (Cp(Mo), C(1)); 155.09 (C═N); 225.99, 238.73 (Mo−C≡O). IR(KBr): ν (cm^{-1}) (intensity): 2015(s), 1927(vs), 1606(w). Mass spectrum: m/z: 600 (M^+).

5.4. X-ray diffraction analyses of **7** and **8**

The intensity data were collected on a CAD-4 diffractometer with a graphite monochromator (Mo-K_α radiation) for complexes **7** and **8**. θ–2θ scan data were collected at room temperature (22 °C). The data were corrected for absorption, Lorentz and polarization effects. The absorption correction is according to the empirical psi rotation. The details of crystal data and intensity collection are summarized in Tables 12 and 13.

The structures were solved by direct methods and were refined by full matrix least squares refinement based on F values. All of the non-hydrogen atoms were refined with anisotropic thermal parameters. All of the hydrogen atoms were positioned at calculated coordinates with a fixed isotropic thermal parameter (U = U (attached atom) + 0.01 $Å^2$). Atomic scattering factors and corrections for anomalous dispersion were from *International Tables for X-ray Crystallography* [27]. All calculations were performed on a PC computer using the SHELEX software package [28].

Table 12
Selected crystal data and structure refinement for **7**.

Identification code	ic3795	
Empirical formula	C17 H14 Mo N4 O7	
Formula weight	482.26	
Temperature	295(2) K	
Wavelength	0.71073 Å	
Crystal system	Triclinic	
Space group	P-1	
Unit cell dimensions	$a = 12.8572(17)$ Å	$\alpha = 65.376(16)°$.
	$b = 13.902(2)$ Å	$\beta = 66.232(14)°$.
	$c = 14.243(3)$ Å	$\gamma = 62.918(12)°$.
Volume	1987.6(6) $Å^3$	
Z	4	
Density (calculated)	1.612 Mg/m^3	
Absorption coefficient	0.706 mm^{-1}	
$F(000)$	968	
Crystal size	0.40 × 0.40 × 0.25 mm^3	
θ range for data collection	1.63–25.00°.	
Index ranges	$-13 \le h \le 15$, $0 \le k \le 16$, $-14 \le l \le 16$	
Reflections collected	6979	
Independent reflections	6979 [R(int) = 0.0000]	
Completeness to $\theta = 25.00°$	100.0%	
Absorption correction	Psi-scan	
Max. and min. transmission	0.8432 and 0.7653	
Refinement method	Full-matrix least-squares on F2	
Data/restraints/parameters	6979/0/525	
Goodness-of-fit on F^2	1.025	
Final R indices [$I > 2\sigma(I)$]	$R1 = 0.0414$, $wR2 = 0.1177$	
R indices (all data)	$R1 = 0.0688$, $wR2 = 0.1302$	
Largest diff. peak and hole	1.224 and −1.105 e $Å^{-3}$	

Table 13
Selected crystal data and structure refinement for **8**.

Identification code	ic3730	
Empirical formula	C22 H20 Mo2 N2 O6	
Formula weight	600.28	
Temperature	295(2) K	
Wavelength	0.71073 Å	
Crystal system	Triclinic	
Space group	P-1	
Unit cell dimensions	$a = 8.5078(17)$ Å	$\alpha = 72.61(3)°$.
	$b = 10.109(2)$ Å	$\beta = 87.79(3)°$.
	$c = 14.495(3)$ Å	$\gamma = 88.66(3)°$.
Volume	1188.7(4) Å3	
Z	2	
Density (calculated)	1.677 Mg/m^3	
Absorption coefficient	1.094 mm^{-1}	
$F(000)$	596	
Crystal size	0.50 × 0.50 × 0.25 mm^3	
θ range for data collection	1.47–24.96°.	
Index ranges	$-10 \le h \le 10$, $0 \le k \le 12$, $-15 \le l \le 17$	
Reflections collected	4160	
Independent reflections	4160 [R(int) = 0.0000]	
Completeness to $\theta = 24.96°$	100.0%	
Absorption correction	Psi-scan	
Max. and min. transmission	0.7717 and 0.6109	
Refinement method	Full-matrix least-squares on F^2	
Data/restraints/parameters	4160/2/281	
Goodness-of-fit on F^2	1.007	
Final R indices [$I > 2\sigma(I)$]	$R1 = 0.0394$, $wR2 = 0.1130$	
R indices (all data)	$R1 = 0.0452$, $wR2 = 0.1179$	
Extinction coefficient	0.0131(12)	
Largest diff. peak and hole	1.089 and −0.679 e $Å^{-3}$	

5.5. Computational method

Calculations based on DFT were carried out using the B3LYP hybrid method involving the three-parameter Becke exchange functional [29] and a Lee–Yang–Parr correlation functional [30]. All calculations were performed using the Gaussian 09 program [31]. The geometries for **4** [20], **7**, and **8** were taken from the crystallographic data. The atomic charges have been analyzed using the Mulliken population analysis.

Acknowledgments

The authors are grateful to the National Science Council of Taiwan for grants in support of this research program and the computational resources provided by the National Center for High-Performance Computing.

References

[1] Y.-P. Wang, X.-H. Lui, B.-S. Lin, W.-D. Tang, T.-S. Lin, J.-H. Liaw, Y. Wang, Y.-H. Liu, J. Organomet. Chem. 575 (1999) 310–319.
[2] D.W. Macomber, M.D. Rausch, Organometallics 2 (1983) 1523–1529.
[3] D.W. Macomber, M.D. Rausch, J. Organomet. Chem. 258 (1983) 331–341.
[4] C. Feher, A. Kuik, L. Mark, L. Kollar, R. Skoda-Foldes, J. Organomet. Chem. 694 (2009) 4036–4041.
[5] M.D. .Rausch, E.A. Mintz, D.W. Macomber, J. Org. Chem. 45 (1980) 689–695.
[6] O.G. Adeyemi, N.J. Coville, Organometallics 22 (2003) 2284–2290.
[7] Y.-P. Wang, J.-M. Hwu, S.-L. Wang, J. Organomet. Chem. 371 (1989) 71–79.
[8] R.M. Silverstein, G.C. Bassler, T.C. Morrill, Spectrometric Identification of Organic Compounds, Wiley, New York, 1981, pp. 117–123.
[9] E.W. Slocum, C.R. Ernst, Adv. Organomet. Chem. 10 (1972) 79–114.
[10] J.B. Stotter, Carbon-13-NMR Spectroscopy, Academic Press, New York, 1972, pp. 197–207.
[11] B.E. Mann, Adv. Organomet. Chem. 12 (1974) 135–213.
[12] A.A. Koridze, P.V. Petrovskii, A.I. Mokhov, A.I. Lutsenko, J. Organomet. Chem. 136 (1977) 57–63.
[13] Y.-P. Wang, P. Wu, H.-Y. Cheng, T.-S. Lin, S.-L. .Wang, J. Organomet. Chem. 694 (2009) 285–296.
[14] Y.-P. Wang, H.-L. Leu, Y. Wang, H.-Y. Cheng, T.-S. Lin, 692 (2007) 3340–3350.

[15] Y.-P. Wang, S.-R. Pang, H.-Y. Cheng, T.-S. Lin, Y. Wang, G.-H. Lee, J. Organomet. Chem. 693 (2008) 329–337.
[16] R. Wang, X. Hong, Z. Shan, Tetrahedron Lett. 49 (2008) 636–639.
[17] L. Barisic, V. Rapic, H. Pritzkow, G. Pavlovic, I. Nemet, J. Organomet. Chem. 682 (2003) 131–142.
[18] D.E. Lewis, J. Chem. Educ. 76 (1999) 1718–1722.
[19] R.D. Rogers, R. Shakir, J.L. Atwood, D.W. Macomber, Y.-P. Wang, M.D. Rausch, J. Crystallogr. Spectrosc. Res. 18 (1988) 767–778.
[20] R.D. Rogers, J.L. Atwood, M.D. Rausch, D.W. Macomer, J. Crystallogr. Spectrosc. Res. 20 (1990) 555–560.
[21] C.M. Lousada, S.S. Pinto, J.N.C. Lopes, M.F.M. da Piedade, H.P. Diogo, M.E.M. da Piedade, J. Phys. Chem. A 112 (2008) 2977–2987.
[22] K. Sato, M. Katada, H. Sano, M. Konno, Bull. Chem. Soc. Jpn. 57 (1984) 2361–2365.
[23] H.E. Amouri, Y. Besace, J. Vaissermann, G. Jaouen, J. Organomet. Chem. 515 (1996) 103–107.
[24] J. Zhao, K.R. Jain, E. Herdtweck, F.E. Kühn, Dalton Trans. (2007) 5567–5571.
[25] S. Barlow, A. Cowley, J.C. Green, T.J. Brunker, T. Hascall, Organometallics 20 (2001) 5351–5359.
[26] Y.-P. .Wang, P. Wu, T.-S. Lin, Polyhedron 42 (2012) 74–83.
[27] J.A. Ibers, W.C. Hamilton (Eds.), International Tables for X-ray Crystallography, vol. IV, Kynoch, Birmingham, England, 1974.
[28] E.J. Gabe, Y.L. Page, J.-P. Charland, F.L. Lee, P.S. White, J. Appl. Crystallogr. 22 (1989) 384–387.
[29] A.D. Becke, J. Chem. Phys. 98 (1993) 5648–5653.
[30] C. Lee, W. Yang, R.G. Parr, Phys. Rev. B 37 (1988) 785–789.
[31] M.J. Frisch, G.W. Trucks, H.B. Schlegel, G.E. Scuseria, M.A. Robb, J.R. Cheeseman, G. Scalmani, V. Barone, B. Mennucci, G.A. Petersson, H. Nakatsuji, M. Caricato, X. Li, H.P. Hratchian, A.F. Izmaylov, J. Bloino, G. Zheng, J.L. Sonnenberg, M. Hada, M. Ehara, K. Toyota, R. Fukuda, J. Hasegawa, M. Ishida, T. Nakajima, Y. Honda, O. Kitao, H. Nakai, T. Vreven, J.A. Montgomery Jr., J.E. Peralta, F. Ogliaro, M. Bearpark, J.J. Heyd, E. Brothers, K.N. Kudin, V.N. Staroverov, R. Kobayashi, J. Normand, K. Raghavachari, A. Rendell, J.C. Burant, S.S. Iyengar, J. Tomasi, M. Cossi, N. Rega, J.M. Millam, M. Klene, J.E. Knox, J.B. Cross, V. Bakken, C. Adamo, J. Jaramillo, R. Gomperts, R.E. Stratmann, O. Yazyev, A.J. Austin, R. Cammi, C. Pomelli, J.W. Ochterski, R.L. Martin, K. Morokuma, V.G. Zakrzewski, G.A. Voth, P. Salvador, J.J. Dannenberg, S. Dapprich, A.D. Daniels, O. Farkas, J.B. Foresman, J.V. Ortiz, J. Cioslowski, D.J. Fox, Gaussian 09, Revision A.02, Gaussian, Inc., Wallingford CT, 2009.